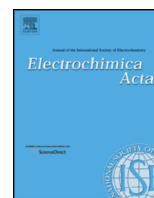




Contents lists available at ScienceDirect

Electrochimica Acta

journal homepage: [www.elsevier.com/locate/electacta](http://www.elsevier.com/locate/electacta)



## Metal-free catalysts for oxygen reduction in alkaline electrolytes: Influence of the presence of Co, Fe, Mn and Ni inclusions

Justus Masa<sup>a,\*</sup>, Anqi Zhao<sup>b</sup>, Wei Xia<sup>b</sup>, Martin Muhler<sup>b</sup>, Wolfgang Schuhmann<sup>a</sup>

<sup>a</sup> Analytische Chemie - Elektroanalytik & Sensorik and Center for Electrochemical Sciences–CES, Ruhr-Universität Bochum, Universitätsstr. 150, D-44780 Bochum, Germany

<sup>b</sup> Laboratory of Industrial Chemistry, Ruhr-Universität Bochum, Universitätsstr. 150, 44780 Bochum, Germany

### ARTICLE INFO

#### Article history:

Received 26 July 2013

Received in revised form 3 November 2013

Accepted 4 November 2013

Available online xxx

#### Keywords:

Metal-free catalysts  
oxygen reduction  
nitrogen modified carbon  
metal inclusions

### ABSTRACT

Metal-free nitrogen modified carbon catalysts (NC) are very closely related to MNC catalysts which contain a transition metal(s) (M), usually Fe or Co as an essential constituent. We investigated the influence of metal inclusions on the activity of nitrogen-doped carbon black in the electrocatalysis of the oxygen reduction reaction (ORR). A reference metal-free NC catalyst was prepared by pyrolysis of a polypyrrole/Vulcan XC72 composite at 800 °C for 2 h under helium. Controlled amounts of Co, Fe, Mn and Ni in low concentrations were then introduced into NC by impregnating it with the corresponding meso-tetra(4-pyridyl) porphyrin metal complex followed by further pyrolysis at 650 °C for 2 h under helium. The resulting catalysts were investigated for ORR using rotating disk electrode and rotating-ring disk electrode voltammetry in 0.1 M KOH. Additionally, the rate of decomposition of hydrogen peroxide by the different catalysts was determined in order to probe the influence of the metal inclusions on the mechanism and selectivity of the ORR. The results show that Fe, Co and Mn inclusions cause a substantial decrease of the overpotential of the reaction and enhance the catalytic current, whereas the presence of Ni has a poisoning effect on ORR. In the presence of Fe, the catalysts apparently reduce oxygen selectively to OH<sup>-</sup> in a direct four electron transfer process as opposed to the two-step, two electron pathway involving hydrogen peroxide as an intermediate for the case of the NC catalyst.

© 2013 Elsevier Ltd. All rights reserved.

### 1. Introduction

Electrocatalysis of oxygen reduction using carbon materials functionalized with nitrogen, phosphorus, boron and sulphur is of topical importance in the field of electrochemical energy conversion and storage, in fuel cells and metal-air batteries [1–4]. The most promising nitrogen modified carbon (NC) catalysts for ORR have been reported in alkaline electrolytes [5,6]. There are several methods for synthesis of metal-free carbon based catalysts for ORR including chemical vapour decomposition (CVD) [7,8], treatment of carbon with a nitrogen plasma [9], pyrolysis of nitrogen rich organic compounds or polymers [10,11], and treatment of carbon with reactive nitrogen rich gases such as ammonia [12], to mention but a few. Some of these methods, for example CVD [7], involve or necessitate the use of metal precursors which have to be removed, mostly by acid leaching, at a later stage of the synthesis. However, the complete removal of metal residues is difficult to prove. Specifically, acid treatment may not fully leach out the residual metal catalysts in carbon nanotubes (CNT) and nitrogen modified carbon

nanotubes (NCNT) prepared using CVD methods [13–18]. Additionally, graphene oxide which is increasingly being used for synthesis of so-called metal-free carbon catalysts modified with heteroatoms [19–21] may be contaminated with manganese impurities [22–25]. This raises the question of whether all the metal-free catalysts claimed in current literature are really free of metal species [26].

Metal-free NC catalysts are closely related to MNC catalysts. The only difference between the two is that the former catalysts are not expected to contain any metal species, whereas, in the latter, a metal, usually Fe or Co is an essential constituent. Generally, pyrolysis of a mixture of carbon and nitrogen rich organic compounds or polymers at high temperatures in the presence of an inert gas or ammonia leads to formation of nitrogen modified carbon with reasonably high activity for ORR [26]. The inclusion of a transition metal precursor in the aforementioned pyrolysis mixture leads to formation of MNC catalysts. Unlike NC, MNC catalysts show very good activity for ORR in acidic electrolytes and are among the most promising non-precious catalysts for oxygen reduction [27–32]. The active sites of MNC catalysts involve metal atoms coordinated to nitrogen, of the form, M-N<sub>x</sub>/C, where x is an integer, mostly 2 or 4 [33,34]. Using CN<sup>-</sup> as a probing ion because of its strong affinity to coordinate to Fe, a decline in the oxygen reduction current of Fe-NC catalysts in the presence of CN<sup>-</sup> was observed thus

\* Corresponding author. Tel.: +49 234 3226202, fax: +49 234 3214683.

E-mail addresses: [justus.masa@rub.de](mailto:justus.masa@rub.de), [masajustus@hotmail.com](mailto:masajustus@hotmail.com) (J. Masa).

adding evidence for the active involvement of Fe in constitution of the active site [35,36]. It is therefore important to understand how metal inclusions, especially in very low concentrations, may affect the ORR activity of NC catalysts in order to avoid misleading designation of metal-free catalysts.

In this study, we investigated the influence of metal inclusions (Co, Fe, Mn and Ni) on the ORR activity of nitrogen modified carbon black in 0.1 M KOH. A reference metal-free nitrogen modified carbon catalyst, denoted NC, was prepared by pyrolysis of a Vulcan/polypyrrole composite at 800 °C under He for 2 h. NC was then impregnated with Co, Fe, Mn and Ni containing *meso*-tetra(4-pyridyl) porphyrins followed by further pyrolysis at 650 °C for 2 h. The ORR activity of the catalysts was investigated using rotating disk electrode (RDE) and rotating-ring disk electrode (RRDE) voltammetry. Furthermore, the rate of decomposition of hydrogen peroxide was measured in order to gain further insight into the influence of the metal inclusions in NC on the mechanism and selectivity of ORR by the different catalysts.

## 2. Experimental Section

### 2.1. Materials

Pyrrole (99% extra pure) was from Acros Organics and was used as received. Anhydrous dichloride salts of Co, Fe, Mn and Ni were from Sigma Aldrich. *Meso*-tetrakis(4-pyridyl)-porphyrin (TPyP) was purchased from Porphyrin Systems. Metallation of TPyP with Co, Fe, Mn and Ni was carried out following a procedure reported earlier [37]. Briefly, TPyP (3 mM) in acetonitrile with the corresponding stoichiometric quantity of anhydrous dichloride metal salts ( $MCl_2$ ) was heated in a reaction tube at 100 °C for two hours under continuous stirring. The products were purified by column chromatography using neutral aluminium oxide (Riedel-de Haën) as the stationary phase and dichloromethane ( $CH_2Cl_2$ ) as the eluent. KOH and acetonitrile were from J. T. Baker. Vulcan XC72 <0.015% metal impurities was a donation from Cabot Corporation. All aqueous solutions were prepared using tri-distilled de-ionized water (SG Water).

### 2.2. Synthesis of polypyrrole/Vulcan XC72 composite

Vulcan carbon XC72 (2 g) was added to Milli-Q water (30 ml) containing acetic acid (10%). The mixture was then ultrasonicated for 15 min. Afterwards, pyrrole equivalent to a mass ratio of 2:5, pyrrole:Vulcan XC72, was added to the suspension followed by further ultrasonication for 20 min. 15 ml of hydrogen peroxide (30%) was then added to the suspension under continuous mixing. The addition of hydrogen peroxide caused spontaneous polymerization of pyrrole. The mixture was further ultrasonicated for 15 min to allow complete polymerization of the pyrrole and its uniform dispersion. The polypyrrole/Vulcan XC72 composite was filtered and dried, first in air for 24 h, then in an oven at 80 °C. It was then placed in a clean quartz boat and pyrolyzed in a horizontal tubular reactor under helium at 800 °C for two h. The resulting powder, denoted NC, was ground to a fine powder and investigated for ORR, or further modified by impregnation with Co, Fe, Mn and Ni *meso*-tetra(4-pyridyl) porphyrins followed by further pyrolysis at 650 °C for 2 h under He.

### 2.3. Incorporation of Co, Fe, Mn and Ni into NC

To introduce Co, Fe, Mn and Ni into NC, the latter was impregnated with a specific amount of the corresponding *meso*-tetrakis(4-pyridyl) porphyrin-metal complex in acetonitrile. The nominal concentration of the metals in NC by weight ranged from

0.05% to 5.0%. The mixtures were homogenised with the aid of ultrasonication for 10 min, dried at 80 °C for 2 h, placed in a quartz glass boat and subsequently pyrolyzed at 650 °C for 2 h under helium gas. The resulting catalysts are denoted as NC/Co, NC/Fe, NC/Mn and NC/Ni for the respective metal inclusions.

### 2.4. Characterization

X-ray photoelectron spectroscopy (XPS) measurements were carried out in an ultra-high vacuum (UHV) set-up equipped with a monochromatic Al K $\alpha$  X-ray source (1486.6 eV; anode operating at 14 kV and 55 mA) and a high resolution Gammadata-Scienta SES 2002 analyzer. The binding energies were calibrated based on the graphite C 1s peak at 284.5 eV. The CASA XPS program with a Gaussian-Lorentzian mixed function and Shirley background subtraction was used to analyze the spectra.

### 2.5. Electrochemical ORR tests

Electrochemical measurements were performed in a Teflon cell using glassy carbon electrodes 0.2475 cm<sup>2</sup> (Pine instruments) modified with the catalysts as the working electrode (WE), a reversible hydrogen electrode (RHE) as the reference electrode (RE) and a Pt wire as the counter electrode (CE). The glassy carbon electrodes were polished on a polishing cloth (LECO) using different alumina pastes (3.0, 1.0, 0.3 and 0.05  $\mu$ m) to obtain a mirror-like surface, followed by ultrasonic cleaning in water. For the preparation of the working electrode, 5.0 mg of the catalyst was dispersed ultrasonically for 30 min in a mixture of water (490  $\mu$ l), ethanol (490  $\mu$ l) and Nafion<sup>®</sup> (5%, 20  $\mu$ l). A specific volume of the resulting catalyst suspension, typically 10.6  $\mu$ l, corresponding to a loading of 0.210 mg cm<sup>-2</sup> was dropped on the polished glassy carbon electrode. The resulting films were left to dry in air and later investigated for ORR by RDE and RRDE voltammetry in 0.1 M KOH using a bipotentiostat/galvanostat (PGSTAT302N, Eco Chemie) in combination with a speed control unit RDE 710 (Gamry Instruments). For RRDE measurements, the collection efficiency was determined for each catalyst film using a Ru<sup>3+</sup>/Ru<sup>2+</sup> (5 mM) redox couple after ORR measurements. All the measurements were carried out at room temperature in the potential range of 1.0 to -0.1 V at a scan rate of 5 mV s<sup>-1</sup> after purging with argon or oxygen for 20 min. The ORR catalytic currents were corrected for background currents by subtracting the current recorded under argon saturation from that recorded under oxygen saturation.

### 2.6. Measurement of the rate of H<sub>2</sub>O<sub>2</sub> disproportionation

To investigate the influence of metal inclusions on the rate of disproportionation of H<sub>2</sub>O<sub>2</sub>, 2  $\mu$ M H<sub>2</sub>O<sub>2</sub> was added to a specific mass of NC or NC/M in a miniaturized electrochemical cell with a total capacity of 1 cm<sup>3</sup>. Chronoamperometric measurements (at 1.1 V vs RHE) were then immediately performed using a disk-shaped Pt ultra microelectrode with a diameter of 25  $\mu$ m to determine the mass transport limited current due to oxidation of H<sub>2</sub>O<sub>2</sub>. All measured currents were normalized against the mass of the catalyst. The temporal concentration of H<sub>2</sub>O<sub>2</sub> was calculated on the basis of the steady-state current  $i = 4nFD C^* r$  at a disk shaped ultra-microelectrode, where  $n$  is the number of electrons transferred ( $n = 2$  for the case of oxidation of H<sub>2</sub>O<sub>2</sub>),  $F$  is the Faraday constant = 96485 C mol<sup>-1</sup>,  $D$  is the diffusion coefficient of H<sub>2</sub>O<sub>2</sub> ( $1.55 \times 10^{-5}$  cm<sup>2</sup> s<sup>-1</sup>, determined in this work using RDE voltammetry),  $C^*$  is the concentration of H<sub>2</sub>O<sub>2</sub> in electrolyte (2  $\mu$ M) and  $r$  is the radius of the disk-shaped ultra microelectrode (12.5  $\mu$ m).

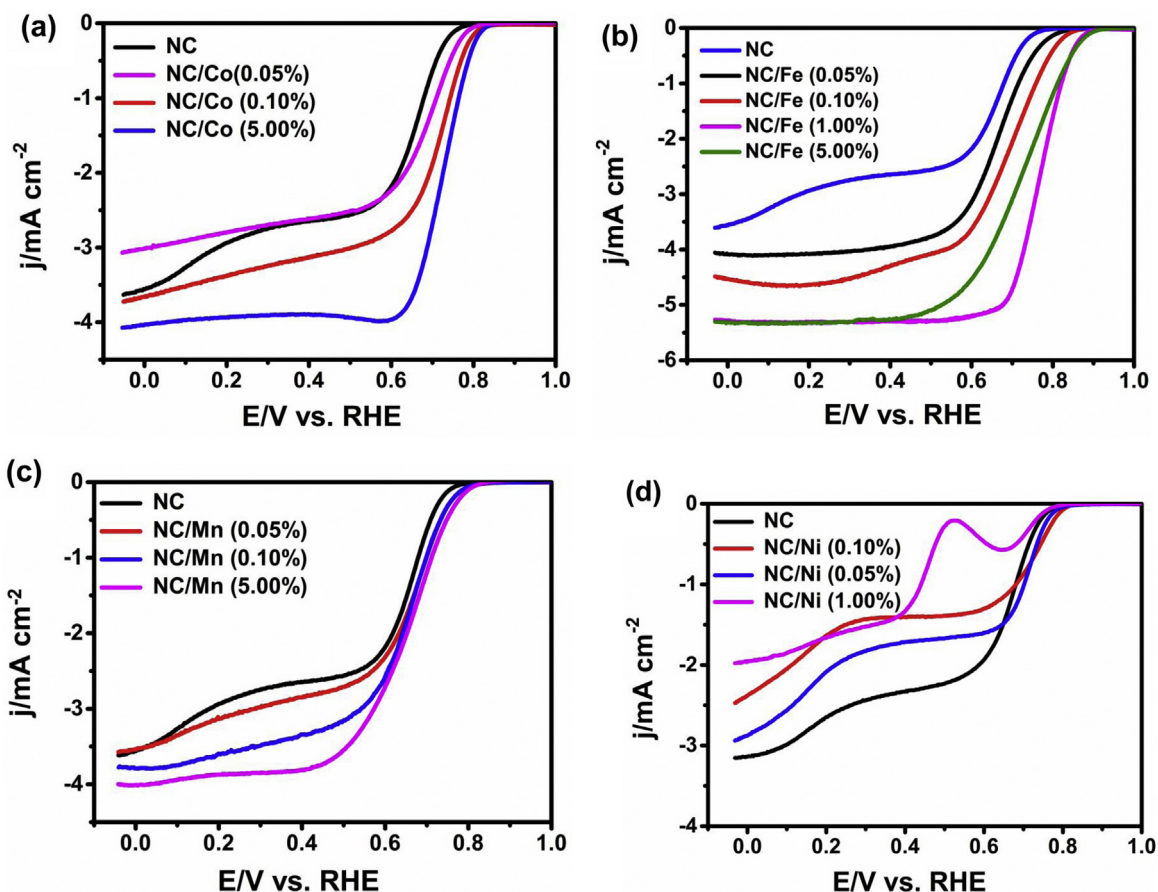


Fig. 1. RDE voltammograms showing the influence of metal inclusions (a) Co, (b) Fe, (c) Mn and (d) Ni at different concentrations on the ORR activity of NC. The scan rate was  $5 \text{ mV s}^{-1}$  and rotation speed of the electrode was 1600 rpm. The percentages represent nominal loading of the metals.

### 3. Results and Discussion

#### 3.1. ORR activity

In alkaline electrolytes, oxygen may be reduced through a direct four electron reduction process to  $\text{OH}^-$  following reaction (i), or through a series  $2e^- \times 2e^-$  process via  $\text{HO}_2^-$  as an intermediate, reactions (ii) and (iii). Alternatively, the  $\text{HO}_2^-$  formed in reaction (ii) may disproportionate to  $\text{OH}^-$  and  $\text{O}_2$  according to reaction (iv). Reactions (iii) and (iv) may proceed concurrently so that the  $\text{O}_2$  formed in (iv) is re-reduced through reaction (ii) followed again by (iii) and (iv) repeatedly until all the  $\text{O}_2$  is converted to  $\text{OH}^-$ . If reactions (iii) and (iv) are very fast, it would then appear as if oxygen is reduced directly to  $\text{OH}^-$  through the four electron transfer process.



The effect of metal inclusions in NC on the activity and selectivity of the ORR was investigated by means of RDE and RRDE voltammetry, and by measurement of the rate of  $\text{H}_2\text{O}_2$  disproportionation. NC was prepared without the involvement of any metal precursors and served as a reference metal-free catalyst. Controlled amounts of Co, Fe, Mn and Ni in the range of 0.05–5.00 wt.% were

then introduced into NC as described in section 2.3 and the resulting effect on ORR activity was investigated. Fig. 1 shows RDE voltammograms of NC/Co, NC/Fe, NC/Mn and NC/Ni for different loadings of the respective metals in NC.

In the absence of any metal species, the case of the NC catalyst, the features of the voltammogram depict a two-step sequential electrochemical process evidenced by the plateau between 0.3 and 0.6 V. This is suggestive of the reduction of oxygen to  $\text{HO}_2^-$  which is then further reduced to  $\text{OH}^-$  at higher overpotentials. The current density in the plateau-like region (0.3–0.6 V) of the NC catalyst was in the range of  $2.4 - 2.7 \text{ mA cm}^{-2}$ , which reasonably corresponds to the diffusion limited current density of  $2.85 \text{ mA cm}^{-2}$  expected for a two-electron transfer process according to Levich's equation,  $i_L = 0.62nFD^{2/3}\nu^{-1/6}C^*$  [38], where  $n$  is the number of electrons transferred,  $D$  is the diffusion coefficient of oxygen in KOH (0.1 M) =  $1.9 \times 10^{-5} \text{ cm}^2 \cdot \text{s}^{-1}$ ,  $C^*$  is the concentration of oxygen in the bulk electrolyte =  $1.2 \times 10^{-6} \text{ mol cm}^{-3}$ ,  $\nu$  is the kinematic viscosity of the electrolyte =  $0.011 \text{ cm}^2 \cdot \text{s}^{-1}$ ,  $F$  is Faraday's constant =  $96485 \text{ C mol}^{-1}$  and  $A$  is the area of the electrode [39]. The slow increase of the current in the second step below 0.3 V indicates that the second process is kinetically slower compared to the first step. Conversely, the  $\text{HO}_2^-$  formed in the first step may undergo disproportionation according to reaction (iv) to form oxygen which is then further reduced to  $\text{HO}_2^-$  in a repeating cycle until all the oxygen is ultimately reduced to  $\text{OH}^-$ . Regardless of the prevailing pathway, the following step(s) are evidently sluggish as manifested by the broad plateau and the slow increase of the current. This was verified using RRDE and by measurement of the rate of disproportionation of hydrogen peroxide as discussed later in subsections 3.3 and 3.4, respectively.

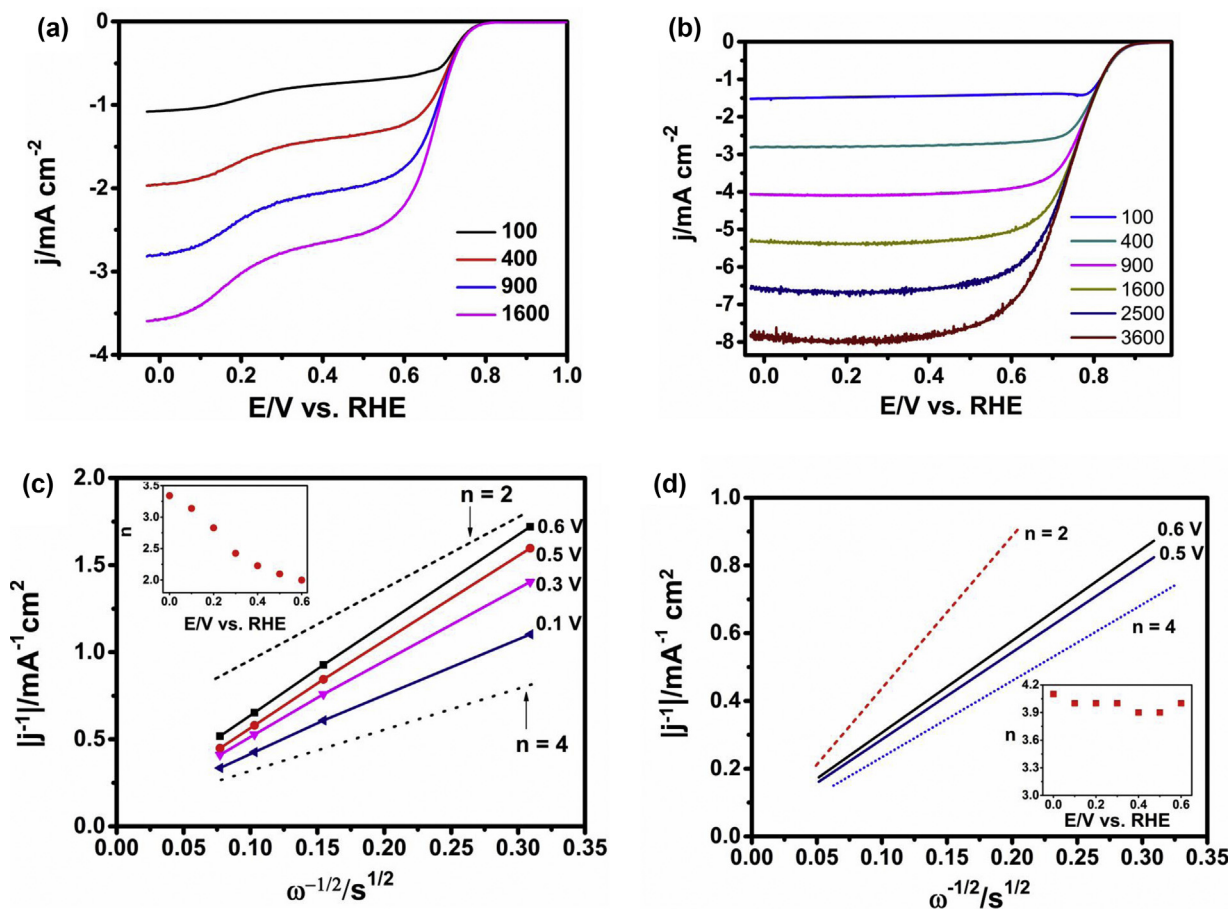


Fig. 2. RDE voltammograms of (a) NC and (b) NC/Fe (1.00%) and the corresponding Koutecky-Levich plots (c) and (d) respectively at different rotation speeds. The insets of 2c and 2d show the calculated number of electrons transferred at different potentials.

With the exception of NC/Ni, the current density scaled with metal content accompanied by a decrease of the overpotential for ORR, even for relatively low metal loadings. The addition of Ni to NC showed an inhibitory effect on the catalytic current. This effect increased with the amount of Ni. Most transition metal oxides and oxy-hydroxides show semi-conducting properties which is disadvantageous for electrocatalysis. We therefore attribute the decline in the ORR current to be partly due to the formation of Ni oxide which was confirmed from XPS studies. At a Ni loading of 1%, two processes can be distinguished. The electrochemical reaction at the higher potential, with a peak at 0.65 V, was also observed when the electrolyte was saturated with argon. Therefore, a group containing Ni should be involved in this reaction and this has a poisoning effect on the ORR activity. Therefore, the presence of Ni in carbon modified catalysts, particularly those modified with nitrogen, has a degenerative effect on the catalytic current.

The presence of Co, Fe and Mn on the ORR activity of NC showed similar tendency. The overpotential for ORR decreased with metal content accompanied by increase of the ORR reduction current. These effects were more pronounced for NC/Fe catalysts.

### 3.2. Rotating disk electrode (RDE) measurements

To get deeper understanding of the influence of the metals on the ORR, RDE voltammetry was used to evaluate the selectivity of the reaction by the different catalysts. From a plot of  $\frac{1}{i}$  against  $\frac{1}{\omega}$  at different rotation speeds on the basis of the Koutecky-Levich equation  $\frac{1}{i} = \frac{1}{i_k} + \frac{1}{B\sqrt{\omega}}$ , where  $B = 0.62nFAD^{2/3}\nu^{-1/6}C^*$  (Levich constant),

and  $i$  and  $i_k$  are the measured and kinetic current respectively, the slope  $(0.62nFAD^{2/3}\nu^{-1/6}C^*)^{-1}$  was used to calculate the number of electrons transferred during the ORR [38].

Fig. 2 shows RDE voltammograms of NC and NC/Fe (1.00%) at different rotation speeds and the corresponding Koutecky-Levich plots at selected potentials. Due to the non-existence of well-defined diffusion limited currents in Fig. 2a, the number of electrons transferred during oxygen reduction by NC varied considerably with the applied potential. This is confirmed in Fig. 2b by the non-parallelism of Koutecky-Levich lines where the slope increases by a factor of about 1.6, from  $3.19 (\text{mA})^{-1} \text{cm}^2 (\text{s}^{-1})^{-1/2}$  at 0.0 V to  $5.18 (\text{mA})^{-1} \text{cm}^2 (\text{s}^{-1})^{-1/2}$  at 0.6 V. Correspondingly, the number of electrons transferred varied with the applied potential as shown in the inset of Fig. 2c. At low overpotentials, above 0.3 V, oxygen is reduced essentially through a two electron process. The number of electrons transferred increases gradually with the applied overpotential to reach 3.5 at 0.0 V. It is therefore very clear that on NC, oxygen is first reduced to  $\text{HO}_2^-$  at low overpotentials, followed by further reduction of  $\text{HO}_2^-$  to  $\text{OH}^-$ . On the contrary, well defined diffusion limited currents were obtained during oxygen reduction by NC/Fe (1.00%) and the reaction proceeded through an apparent direct four electron transfer process at all the potentials as shown by the inset in Fig. 2d. Additionally, the diffusion limited current obtained with NC/Fe is close to the theoretical current according to Levich's equation at all rotation speeds. The apparent four-electron reduction of oxygen by NC/Fe (1.00%) indicates that if at all oxygen is first reduced to  $\text{HO}_2^-$  by this catalyst, then, the following reaction(s), either (iii) or (iv), or both of them are very facile. Since the calculated number of electrons ( $n$ ) transferred on the basis

**Table 1**  
Kinetic parameters showing the influence of metal inclusions in NC on the ORR.

Catalyst	Nominal metal content (wt.%)	Rate of H <sub>2</sub> O <sub>2</sub> decomposition (μM/s)	Number of electrons at 0.4 V <sup>a</sup>	H <sub>2</sub> O <sub>2</sub> (%) at 0.4 V <sup>a</sup>
NC	–	0.013	2.3	39.4
NC/Co	0.05	–	2.6	26.4
	0.10	–	3.1	21.1
	5.00	–	3.5	16.8
NC/Fe	0.05	0.017	3.4	20.2
	0.10	0.022	3.8	12.3
	1.00	0.025	3.9	9.6
NC/Mn	0.05	0.009	2.5	33.4
	0.10	0.009	3.2	27.2
	1.00	0.016	3.6	23.9
NC/Ni	0.10	0.011	2.2	39.0

<sup>a</sup> Potential vs. RHE.

of the Koutecky-Levich analysis varied with the applied potential, as shown by the examples of the insets in Fig. 2b and Fig. 2d, the average number of electrons transferred during ORR by the different catalysts was compared at 0.4 V as summarized in Table 1. At a metal loading of 0.05%, both NC/Co ( $n = 2.6$ ) and NC/Mn ( $n = 2.5$ ) reduce oxygen more selectively to HO<sub>2</sub><sup>-</sup>, however, the intermediate plateau-like feature characteristic of NC disappeared for the case of NC/Co, while it became less pronounced for NC/Mn. This indicates that reaction (iii) or (iv), or both, proceed faster than in the case of NC. At a similar loading, NC/Fe ( $n = 3.4$ ) apparently reduces oxygen more selectively to OH<sup>-</sup> through reaction (i), or through reaction (ii) followed by reactions (iii) and (iv) which proceed very fast as already shown for NC/Fe (1.0%) above. Higher loadings of Co and Mn seem to favour reaction (i), or to increase the kinetics of reaction (iii) and (iv). The number of electrons transferred as calculated from RDE data is only suggestive of the prevailing pathway for

ORR. It is not possible to definitively conclude whether the reaction proceeds exclusively through reaction (i), or first through reaction (ii) followed by rapid co-occurrence of reactions (iii) and (iv). We therefore carried out RRDE measurements and hydrogen peroxide decomposition measurements in order to gain clearer understanding of the exact prevailing reaction pathway.

### 3.3. Rotating-ring disk electrode (RRDE) measurements

The influence of metal inclusions in NC on the selectivity of ORR was further investigated by RRDE voltammetry, and by measurement of the rate of chemical decomposition of H<sub>2</sub>O<sub>2</sub> as summarized in Fig. 3.

The ring collection efficiency ( $N$ ) of the RRDE,  $N = -i_R/i_D$ , where  $i_R$  is the ring current and  $i_D$  is the disk current, was determined for each individual catalyst film after ORR measurements using a

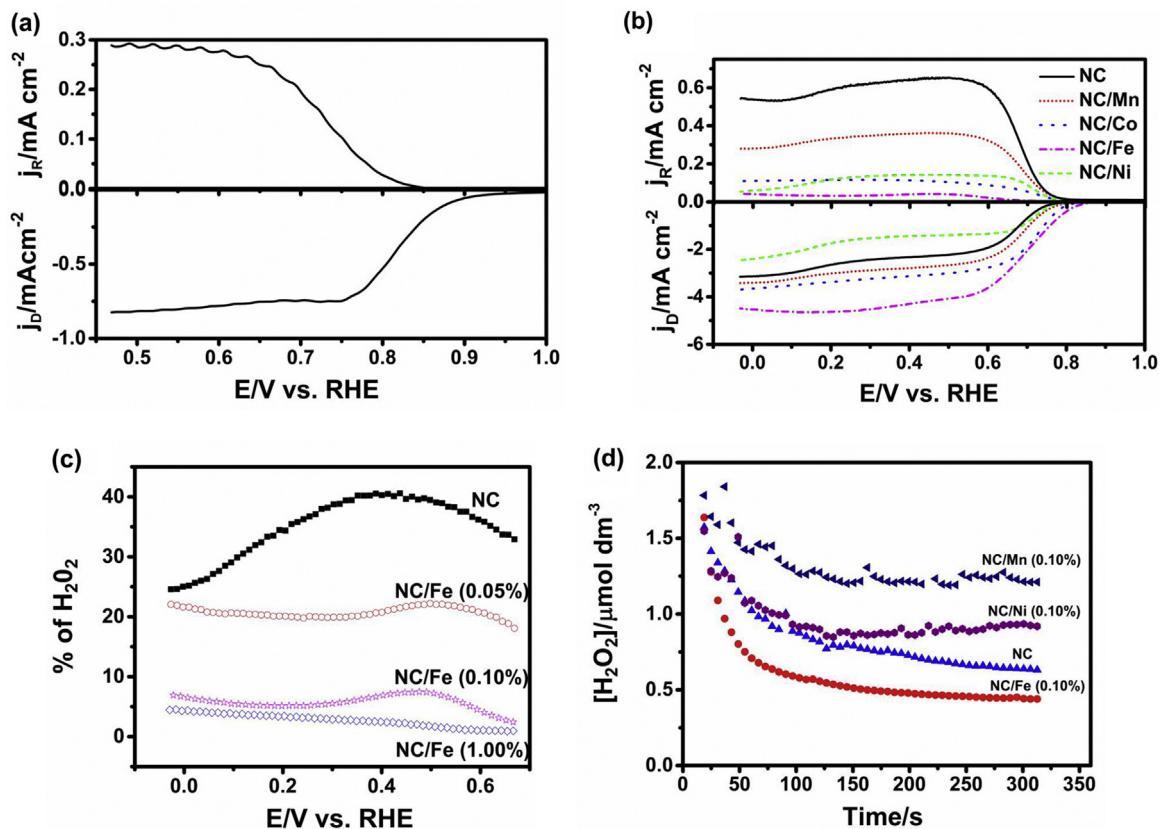


**Fig. 3.** (a) RRDE voltammograms showing the reduction of Ru<sup>3+</sup> to Ru<sup>2+</sup> at the disk modified with NC (scan rate = 5 mV s<sup>-1</sup>, rotation speed = 1600 rpm), and the oxidation of Ru<sup>2+</sup> to Ru<sup>3+</sup> at the ring. (b) RRDE voltammograms showing oxygen reduction at the disk modified with NC, NC/Co (0.1%), NC/Fe (0.1%), NC/Mn (0.1%) and NC/Ni (0.1%) and H<sub>2</sub>O<sub>2</sub> oxidation at the Pt ring, (c) Percentage of H<sub>2</sub>O<sub>2</sub> generated as a function of the loading of Fe in NC, (d) chemical decomposition of H<sub>2</sub>O<sub>2</sub> by NC, NC/Fe, NC/Mn and NC/Ni.

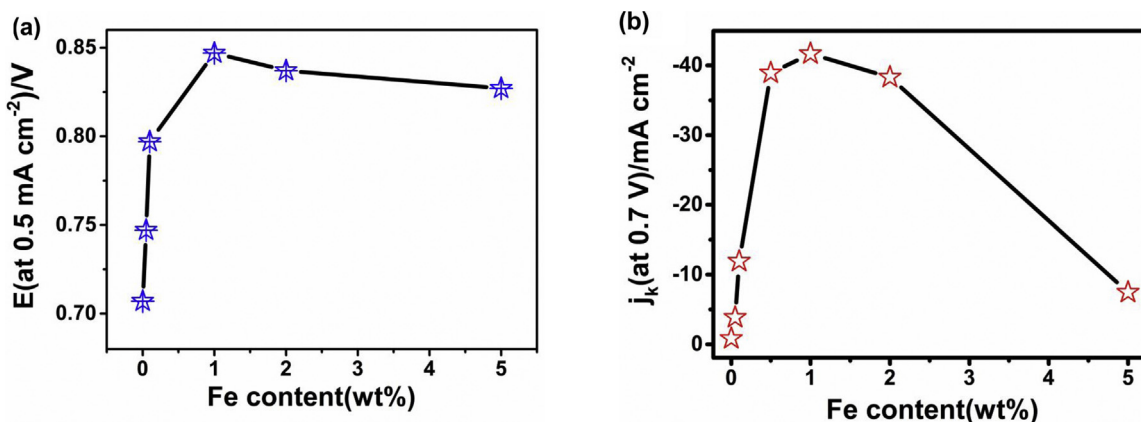


Fig. 4. (a) Variation of the onset potential for ORR with Fe loading, (b) variation of the kinetic current at 0.7 V with Fe loading.

solution of hexamineruthenium (III) chloride (5 mM) in the same electrolyte used for ORR measurements. Fig. 3a shows an experiment for determination of the ring collection efficiency for a NC catalyst film, which was in this particular case 26.4%. The value of  $N$  provided by the supplier is 37%, which applies to smooth surfaces. The collection efficiency of the catalysts generally ranged from 18.4 to 27.8%.

Fig. 3b shows a summary of the dependency of  $\text{HO}_2^-$  generation on the type of metal present in NC, at a loading of 0.1%. The percentage of  $\text{HO}_2^-$  generated was calculated from the RRDE equation,  $\text{H}_2\text{O}_2(\%) = (200I_R/N)/(I_D + (I_R/N))$  [40], where  $N$ ,  $I_R$  and  $I_D$  retain their meanings as defined above. At low overpotentials, the percentage of  $\text{HO}_2^-$  generated by NC was in the range of 30–45% and it decreased to about 25% at higher overpotentials. The percentage of  $\text{HO}_2^-$  generated by the different catalysts was compared at 0.4 V resulting in 16.8% for NC/Co (0.1%), 9.6% for NC/Fe (0.1%), 23.9% for NC/Mn (0.1%) and 39.0% for NC/Ni (0.1%). The high amount of  $\text{H}_2\text{O}_2$  generated by NC/Mn and NC/Ni suggests that ORR on these catalysts proceeds mainly through reaction (ii) followed by either (iii), or (iv), or both (iii) and (iv) concurrently. Therefore, in contrast to the RDE results, we see here that reaction (i) cannot be the dominant reaction for the case of NC/Mn (0.1%) due to the substantial amount of  $\text{HO}_2^-$  generated. Additionally, the results also indicate that NC/Mn and NC/Ni are poor catalysts for  $\text{HO}_2^-$  reduction or disproportionation.

#### 3.4. Rate of $\text{H}_2\text{O}_2$ disproportionation

Fig. 3d shows a representative example of the concentration of  $\text{H}_2\text{O}_2$  with time for 300 s.

Because the rate of  $\text{H}_2\text{O}_2$  disproportionation becomes significantly reduced, or reaches a steady state after about 100 s, the change in concentration of the  $\text{H}_2\text{O}_2$  during the initial 50 s was used to calculate its rate of disproportionation and the results are summarized in Table 1. It was not possible to determine the rate of disproportionation of NC/Co by this method because of apparent side reactions manifested by unexpected increase of the current with time. We suppose that in the course of disproportionation of  $\text{H}_2\text{O}_2$ ,  $\text{Co}^{2+}$  species are oxidized to  $\text{Co}^{3+}$  such that during the chronoamperometric measurements at 1.1 V vs RHE, homogeneous redox reactions in the electrolyte produce species which are also oxidized at the electrode alongside  $\text{H}_2\text{O}_2$  thus leading to unexpected increase of the observed current.

NC was found to disproportionate  $\text{H}_2\text{O}_2$  faster than both NC/Mn (0.1%) and NC/Ni (0.1%). For example, the rate of disproportionation of  $\text{H}_2\text{O}_2$  by NC/Mn ( $0.009 \mu\text{M s}^{-1}$ ), is about 1.4 times slower compared to NC ( $0.013 \mu\text{M s}^{-1}$ ). At least 68.5% of the  $\text{H}_2\text{O}_2$  had been disproportionated by NC after 300 s compared to 39.5% by NC/Mn, 78% by NC/Fe and 54% by NC/Ni during the same time. These observations lead us to conclude that after the initial two electron reduction of  $\text{O}_2$  to  $\text{HO}_2^-$  on NC (reaction (ii)), the peroxide formed undergoes disproportionation to form oxygen (reaction (iv)) which is subsequently reduced again to  $\text{HO}_2^-$ . This cycle is likely to continue until all the oxygen is reduced to  $\text{OH}^-$ . Reactions (ii) and (iv) seem to proceed in parallel with reaction (iii) although it is not clear which one of these steps is dominant. The slow disproportionation of  $\text{H}_2\text{O}_2$  by NC/Mn and NC/Ni means that reaction (iv) does not play a major role during oxygen reduction by these catalysts. For these catalysts, since the diffusion limited current is significantly lower than that predicted by Levich's equation,  $5.7 \text{ mA cm}^{-2}$

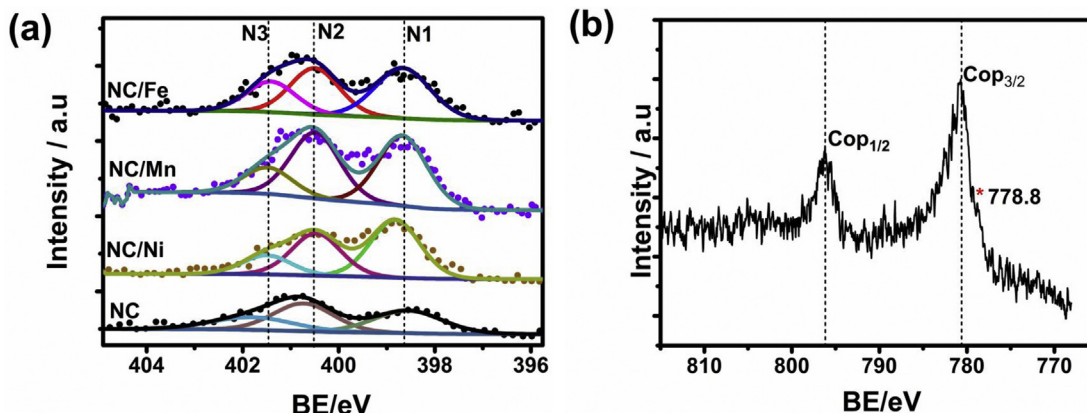


Fig. 5. (a) High resolution N 1s spectra of NC, NC/Fe, NC/Mn and NC/Ni, (N1 = pyridinic, N2 = pyrrolic and N3 = graphitic), (b) 2p core-level spectra of cobalt in NC/Co.

at a rotation speed of 1600 rpm, reaction (i) cannot be the major reaction. Therefore, on NC/Mn and NC/Ni, oxygen seems to be mainly reduced to  $\text{HO}_2^-$  followed by further reduction of  $\text{HO}_2^-$  to  $\text{OH}^-$ . However, this proposition does not preclude the parallel prevalence of the direct four-electron transfer pathway; it is only an indication that the reaction proceeds much slower. The mechanism of ORR on NC/Fe is not straight forward. RRDE results show minimal generation of  $\text{H}_2\text{O}_2$  by NC/Fe, and Koutecky-Levich analysis shows that the reaction proceeds through an apparent direct four electron transfer process. On the other hand,  $\text{H}_2\text{O}_2$  disproportionation measurements show that the disproportionation of  $\text{H}_2\text{O}_2$  on NC/Fe is considerably very fast compared to NC. Therefore, it is equally likely that either reaction (i) is dominant, or that the reaction proceeds via  $\text{HO}_2^-$  as an intermediate followed by its disproportionation (fast reaction) and further reduction of the formed oxygen leading to an apparent four electron transfer process.

### 3.5. Effect of Fe loading on ORR activity

The low amount of  $\text{H}_2\text{O}_2$  generated by NC/Fe motivated us to investigate the influence of Fe loading on  $\text{H}_2\text{O}_2$  generation as summarized in Fig. 3c. The maximum amount of  $\text{HO}_2^-$  generated by NC/Fe decreased with the Fe content from about 20% for NC/Fe (0.05%), to 12% for NC/Fe (0.1%) and  $< 10\%$  for NC/Fe (1.0%). It may therefore be concluded that the amount of  $\text{H}_2\text{O}_2$  generated is low for high loadings of Fe in NC. However, we see from Fig. 1b that the ORR activity of NC/Fe increases with Fe loading up to about 1.0% and then begins to decline. To get a clearer picture of how Fe inclusions affect the selectivity and ORR activity of NC, we investigated the influence of Fe loading on the kinetic current and the onset for ORR as summarized in Fig. 4.

The onset potential (the potential corresponding to a current density of  $0.1 \text{ mAcm}^{-2}$ ) for ORR initially increases sharply to a maximum at a loading of about 1.0% and then decreases gradually at higher Fe loadings (Fig. 4a). Similarly, the kinetic current at 0.7 V of the NC/Fe catalysts increases sharply with Fe loading to a maximum at about 1% then decreases at higher loadings. These observations are consistent with studies by other groups [34,41] and they highlight the important fact that very small amounts of Fe in NC can significantly promote the ORR. Wang et al. found the activity of Fe-NC catalysts to increase with Fe content from 10 to 1000 ppm, and then decline at higher Fe concentrations [42]. The active site(s) of MNC catalysts containing Fe are believed to involve Fe coordinated to N [41,42]. Metallic Fe, and oxides of Fe are not known to be active for oxygen reduction. Therefore, only Fe coordinated to N is believed to promote the ORR activity of the NC catalyst, and the optimal content of Fe would be that which is just enough to coordinate all the nitrogen atoms. An excess amount of Fe in the precursor would cause sintering of uncoordinated Fe upon heating and the possible formation of Fe oxides, both of which do not

**Table 2**

Nitrogen content and relative intensity of nitrogen functional groups.

Catalyst	Nitrogen content (%)	Relative abundance (%)		
		pyridinic	pyrrolic	quaternary
NC	3.23	39.3	42.5	18.2
NC/Fe	2.34	42.4	34.8	22.9
NC/Mn	3.13	43.2	40.5	16.3
NC/Ni	3.02	48.6	35.4	16.1

promote ORR activity thus leading to the observed decline of ORR activity.

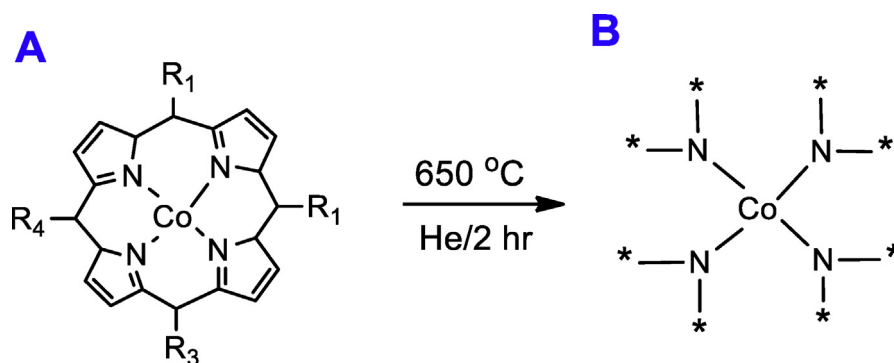
### 3.6. Correlation between chemical composition and ORR activity

X-ray photoelectron spectroscopy (XPS) was used to investigate the relationship between the chemical composition and structure of the catalysts and their electrochemical behavior. Nitrogen functionalized carbon groups, specifically, graphitic, pyridinic and pyrrolic are claimed to be responsible for the ORR activity of NC catalysts [43]. If oxygen reduction depends exclusively on the presence of these groups, it should be possible to explain the ORR activity of the catalysts both qualitatively and quantitatively in terms of these groups. Fig. 5a shows deconvoluted high resolution N 1s spectra of NC, NC/Fe, NC/Mn and NC/Ni in which the nominal loading of the respective metals was 0.1%.

Qualitatively, the catalysts contained the same nitrogen functional groups, namely, pyridinic (N1), pyrrolic (N2) and graphitic (N3). However, the relative intensities of N1, N2 and N3 were different in all the catalysts as summarized in Table 2.

The present results show that the ORR activity of the catalysts cannot be attributed to a single functional group. The results are consistent with our previous studies where we observed that the ORR activity of NC catalysts was neither correlated with the total nitrogen content of the catalysts nor with any particular nitrogen functional group. However, a fairly linear correlation was found between the onset potential for ORR and the combined relative intensity of pyridinic (N1) and graphitic (N3) nitrogen [12]. It is therefore difficult to explain the factors responsible for enhancement of activity due to the presence of the metal inclusions in terms of nitrogen functional groups.

There is evidence from time-of-flight mass spectrometry (ToF MS) of the presence of  $\text{FeN}_4\text{C}$  and  $\text{FeN}_2\text{C}$  groups in MNC catalysts containing Fe which have been suggested to be involved as active sites during oxygen reduction [33]. The formation of Fe-N bonds has also been observed using extended x-ray absorption fine structure (EXAFS) studies [44]. Additionally, using  $^{56}\text{Fe}$  Mössbauer spectroscopy, Koslowski et al. observed a positive correlation between  $\text{FeN}_4\text{C}$ - groups and the selectivity of the Fe-NC catalysts towards  $\text{H}_2\text{O}$  [45]. On the other hand, in addition to the



**Scheme 1.** Suggested scheme for the degradation of a substituted cobalt porphyrin during pyrolysis at  $650^\circ\text{C}$  under helium. The symbol (\*) represents a carbon atom.

formation of cobalt oxide species, we observed evidence of Co-N bonds in NC/Co catalysts from the Co 2p core level spectra of NC/Co catalysts, as shown by the shoulder at 778.8 eV in Fig. 5b. This finding is in accordance with several studies where it has been suggested that the Co-N<sub>4</sub> core of cobalt-N<sub>4</sub> macrocyclic complexes is preserved for pyrolysis of the complexes at moderate temperatures 600–700 °C, as represented in Scheme 1 [46,47]. Separate studies have also suggested that the Co-N<sub>4</sub> moiety is formed during pyrolysis of a mixture of a nitrogen rich organic compound or polymer and a suitable cobalt salt supported on carbon [48–50]. Transition metal oxides, for example the mixed Co<sub>3</sub>O<sub>4</sub> [51] and Mn<sub>3</sub>O<sub>4</sub> [52] oxides supported on graphitic carbon exhibit reasonably high activity for oxygen reduction. Therefore, based on our observations and on the experimental evidence by others, the participation of metal containing groups as active sites for ORR in NC catalysts cannot be ruled out. Further to this, given the closeness between MNC and NC catalysts, the designation of metal-free catalysts has to be done carefully bearing in mind that metal inclusions even in relatively low concentrations can significantly affect ORR activity.

#### 4. Conclusions

In this study, the influence of metal inclusions (Co, Fe, Mn and Ni) on the activity of nitrogen modified carbon catalysts (NC) was investigated. With the exception of NC/Ni, the current density scaled with metal content with a corresponding decrease of the overpotential for ORR, even for very low metal loadings, particularly more pronounced for the case of NC/Fe. The addition of Ni to NC showed an inhibitory effect on the catalytic current. The amount of H<sub>2</sub>O<sub>2</sub> generated decreased in the order NC (39.4%) > NC/Ni (39.0%) > NC/Mn (23.9%) > NC/Co (16.8%) > NC/Fe (9.6%), at a metal loading of 0.1%. An apparent direct four-electron transfer pathway was only observed for the reduction of oxygen by NC/Fe. The rest of the catalysts, NC, NC/Co, NC/Mn and NC/Ni reduced oxygen via the peroxide (HO<sub>2</sub><sup>-</sup>) intermediate. H<sub>2</sub>O<sub>2</sub> disproportionation measurements showed that only NC/Fe has a higher rate of H<sub>2</sub>O<sub>2</sub> disproportionation than NC. H<sub>2</sub>O<sub>2</sub> disproportionation was shown to be an important reaction pathway for the reduction of oxygen to OH<sup>-</sup> by NC catalysts.

#### Acknowledgements

The authors are grateful for financial support in the framework of the Helmholtz Energieallianz. A. Zhao thanks the China Scholarship Council for a research grant.

#### References

- [1] D. Yu, E. Nagelli, F. Du, L. Dai, *J. Phys. Chem. Lett.* 1 (2010) 2165–2173.
- [2] C.H. Choi, M.W. Chung, H.C. Kwon, S.H. Park, S.I. Woo, *J. Mater. Chem. A* 1 (2013) 3694.
- [3] J. Liang, Y. Jiao, M. Jaroniec, S.Z. Qiao, *Angew. Chem. Int. Ed.* 51 (2012) 11496.
- [4] D.-S. Yang, D. Bhattacharjya, S. Inamdar, J. Park, J.-S. Yu, *J. Am. Chem. Soc.* 134 (2012) 16127.
- [5] Z. Yang, H. Nie, X. Chen, X. Chen, S. Huang, *J. Power Sources*, 236 (2013) 238.
- [6] W.Y. Wong, W.R.W. Daud, A.B. Mohamad, A.A.H. Kadhum, K.S. Loh, E.H. Majlan, *Int. J. Hydrogen. Energy* 38 (2013) 9370.
- [7] K. Gong, F. Du, Z. Xia, M. Durstock, L. Dai, *Science* 323 (2009) 760–764.

- [8] N. Alexeyeva, E. Shulga, V. Kisand, I. Kink, K. Tammeveski, *J. Electroanal. Chem.* 648 (2013) 169.
- [9] J.G. Jones, A.R. Waite, C. Muratore, A.A. Voevodin, *J. Vac. Sci. Technol. B* 26 (2008) 995.
- [10] W. Xia, J. Masa, M. Bron, W. Schuhmann, M. Muhler, *Electrochem. Commun.* 13 (2011) 593.
- [11] M. Vikkisk, I. Kruusenberg, U. Joost, E. Shulga, K. Tammeveski, *Electrochim. Acta* 87 (2013) 709.
- [12] A. Zhao, J. Masa, M. Muhler, W. Schuhmann, W. Xia, *Electrochim. Acta* 98 (2013) 139.
- [13] B. Štjukić, C.E. Banks, R.G. Compton, *Nano Lett.* 6 (2006) 1556–1558.
- [14] K. Jurkschat, X. Ji, A. Crossley, R.G. Compton, C.E. Banks, *Analyst* 132 (2006) 21.
- [15] C.E. Banks, A. Crossley, C. Salter, S.J. Wilkins, R.G. Compton, *Angew. Chem. Int. Ed.* 45 (2006) 2533.
- [16] M. Pumera, H. Iwai, *J. Phys. Chem. C* 113 (2009) 4401.
- [17] M. Pumera, H. Iwai, *Chem. Asian J.* 4 (2009) 554.
- [18] M. Pumera, *Langmuir* 23 (2007) 6453.
- [19] Z. Lin, G. Waller, Y. Liu, M. Liu, C.-p. Wong, *Adv. Energy Mater.* 2 (2012) 884.
- [20] Z.-H. Sheng, L. Shao, J.-J. Chen, W.-J. Bao, F.-B. Wang, X.-H. Xia, *ACS Nano* 5 (2011) 4350.
- [21] S. Yang, X. Feng, X. Wang, K. Müllen, *Angew. Chem. Int. Ed.* 50 (2011) 5339.
- [22] A.M. Panich, A.I. Shames, N.A. Sergeev, *Appl Magn Reson.* 44 (2013) 107.
- [23] A.M. Panich, A.I. Shames, A.E. Aleksenskii, A. Dideikin, *Solid State Commun.* 152 (2012) 466.
- [24] A. Ambrosi, S.Y. Chee, B. Khezri, R.D. Webster, Z. Sofer, M. Pumera, *Angew. Chem. Int. Ed.* 51 (2012) 500.
- [25] A. Ambrosi, C.K. Chua, B. Khezri, Z. Sofer, R.D. Webster, M. Pumera, *Proc. Natl. Acad. Sci. USA* 109 (2012) 12899.
- [26] H.-S. Oh, H. Kim, *J. Power Sources* 212 (2012) 220.
- [27] H. Peng, Z. Mo, S. Liao, H. Liang, L. Yang, F. Luo, H. Song, Y. Zhong, B. Zhang, *Sci. Rep.* 3 (2013) 1.
- [28] H.T. Chung, J.H. Won, P. Zelenay, *Nat. Commun.* 4 (2013) 1922.
- [29] T. Schilling, A. Okunola, J. Masa, W. Schuhmann, M. Bron, *Electrochim. Acta* 55 (2010) 7597.
- [30] F. Jaouen, E. Proietti, M. Lefevre, R. Chenitz, J.-P. Dodelet, G. Wu, H.T. Chung, C.M. Johnston, P. Zelenay, *Energy Environ. Sci.* 4 (2011) 114.
- [31] M. Lefevre, E. Proietti, F. Jaouen, J.-P. Dodelet, *Science* 324 (2009) 71.
- [32] G. Wu, K.L. More, C.M. Johnston, P. Zelenay, *Science* 332 (2011) 443.
- [33] M. Lefevre, J.P. Dodelet, P. Bertrand, *J. Phys. Chem. B* 106 (2002) 8705.
- [34] M. Lefevre, J.P. Dodelet, P. Bertrand, *J. Phys. Chem. B* 104 (2000) 11238.
- [35] Y. Li, W. Zhou, H. Wang, L. Xie, Y. Liang, F. Wei, J.-C. Idrobo, S.J. Pennycook, H. Dai, *Nat. Nanotechnol.* 7 (2012) 394.
- [36] W. Li, J. Wu, D.C. Higgins, J.-Y. Choi, Z. Chen, *ACS Catal.* 2 (2012) 2761.
- [37] J. Masa, W. Schuhmann, *Chem. Eur. J.* 19 (2013) 9644.
- [38] A.J. Bard, L.R. Faulkner, *Electrochemical methods: Fundamentals and applications*, 2nd ed., Wiley, New York, 2001.
- [39] A. Parthasarathy, S. Srinivasan, A.J. Appleby, C.R. Martin, *J. Electrochem. Soc.* 139 (1992) 2530.
- [40] U.A. Paulus, T.J. Schmidt, H.A. Gasteiger, R.J. Behm, *J. Electroanal. Chem.* 495 (2001) 134.
- [41] J. Wang, G. Yin, Y. Shao, S. Zhang, Z. Wang, Y. Gao, *J. Power Sources* 171 (2007) 331.
- [42] H. Wang, R. Côté, G. Faubert, D. Guay, J.P. Dodelet, *J. Phys. Chem. B* 103 (1999) 2042.
- [43] N.P. Subramanian, X. Li, V. Nallathambi, S.P. Kumaraguru, H. Colon-Mercado, G. Wu, J.-W. Lee, B.N. Popov, *J. Power Sources* 188 (2009) 38–44.
- [44] H.R. Byon, J. Suntivich, Y. Shao-Horn, *Chem. Mat.* 23 (2011) 3421.
- [45] U.I. Koslowski, I. Abs-Wurmbach, S. Fiechter, P. Bogdanoff, *J. Phys. Chem. C* 112 (2008) 15356.
- [46] M. Yuasa, A. Yamaguchi, H. Itsuki, K. Tanaka, M. Yamamoto, K. Oyaizu, *Chem. Mat.* 17 (2005) 4278–4281.
- [47] T.S. Olson, S. Pylypenko, P. Atanassov, K. Asazawa, K. Yamada, H. Tanaka, *J. Phys. Chem. C* 114 (2010) 5049.
- [48] Z. Shi, H. Liu, K. Lee, E. Dy, J. Chlistunoff, M. Blair, P. Zelenay, J. Zhang, Z.-S. Liu, *J. Phys. Chem. C* 115 (2011) 16672.
- [49] J. Masa, T. Schilling, M. Bron, W. Schuhmann, *Electrochim. Acta* 60 (2012) 410–418.
- [50] J. Masa, A. Zhao, W. Xia, Z. Sun, B. Mei, M. Muhler, W. Schuhmann, *Electrochem. Commun.* 34 (2013) 113–116.
- [51] Y. Liang, Y. Li, H. Wang, J. Zhou, J. Wang, T. Regier, H. Dai, *Nat. Mater.* 10 (2011) 780.
- [52] Y. Tan, C. Xu, G. Chen, X. Fang, N. Zheng, Q. Xie, *Adv. Funct. Mater.* 22 (2012) 4584.